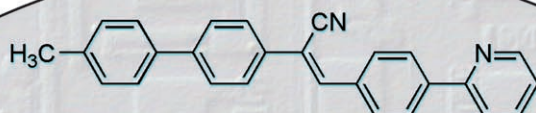


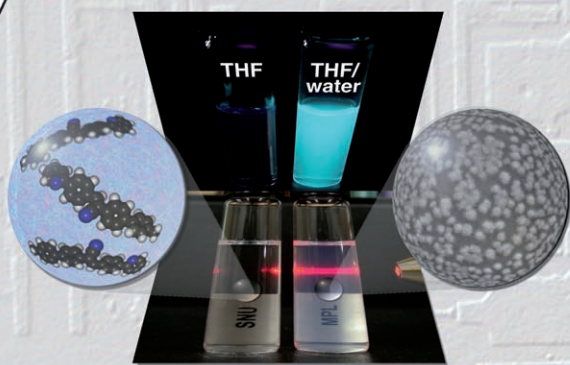
# Photopatterned Arrays of Fluorescent Organic Nanoparticles\*\*

Byeong-Kwan An, Soon-Ki Kwon, and Soo Young Park\*

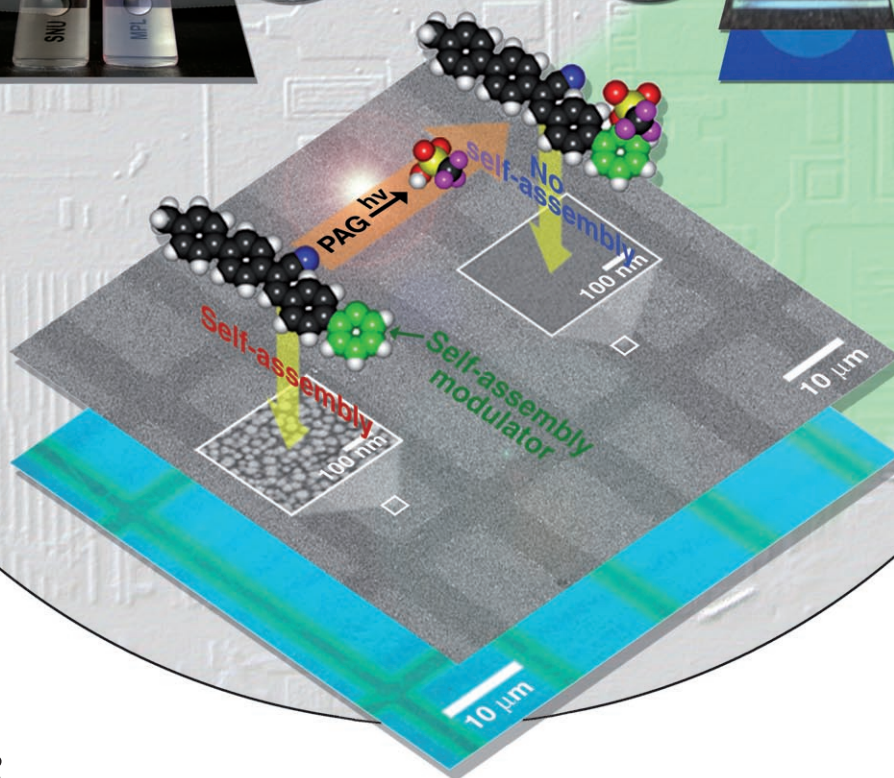
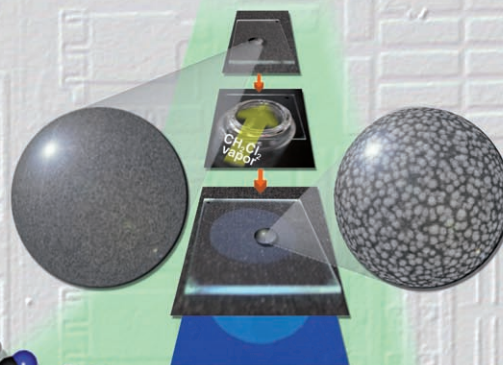


## Fluorescent Organic Nanoparticles (FONs) Preparation

Reprecipitation method:  
FONs in suspension solution



VDSA method:  
FONs in polymer matrix



Fluorescent organic nanoparticles (FONs) have become the subject of ever-increasing attention in recent years, as a result of their large diversity in molecular structure and optical properties that are of potential use in optoelectronics and biologics.<sup>[1–11]</sup> This research has, to date, principally focused on colloidal-state FONs, which can readily be prepared with simple reprecipitation methods<sup>[1–12]</sup> (also known as the Ouzo effect).<sup>[13]</sup> To explore the collective properties of FONs as well as to realize practical device applications, however, reliable methods of transferring and aligning them with large surface areas on solid substrates are required. Electrophoretic deposition,<sup>[14]</sup> lithographic patterning,<sup>[15]</sup> and ink-jet printing<sup>[16]</sup> of organic/inorganic nanoparticles have been proposed as methods appropriate to this purpose. As all these methods are based on the strategy of transferring preformed FONs onto the substrate, which demands separate nanoparticle synthesis and complicated handling, we decided to explore the possibility of FON array fabrication, that is, the in situ generation of FONs on a polymer film. Herein, we report a promising new approach to the fabrication of photopatterned FON arrays, which is based on the principles of vapor-driven self-assembly (VDSA) and patternwise photoacid generation.

The VDSA process is based on the selective phase demixing and self-assembled aggregate formation that occurs from a molecularly dispersed solid solution of specific fluorescent molecules in a polymer matrix when it is exposed to volatile organic solvent vapors. For the implementation of the VDSA process, we designed and synthesized a fluorescent molecule, 1-cyano-*trans*-1-(4'-methylbiphenyl)-2-[4'-(2'-pyridyl)phenyl]ethylene (Py-CN-MBE; Figure 1), which has a strong self-assembling capability as well as a functional pyridine group that can respond to in situ generated photoacid. Py-CN-MBE is structurally similar to the non-pyridine analogue 1-cyano-*trans*-1,2-bis-(4'-methylbiphenyl)ethylene (CN-MBE).<sup>[4]</sup> This molecule has been shown to have a strong nanoparticle formation capability through self-assembly with concomitant fluorescence turn-on (so-called aggregation-induced enhanced emission (AIEE)),<sup>[4,5,17]</sup> which is useful for the direct visualization of the VDSA event because the fluorescence of the molecule changes instantly when nanoparticles are generated.

Py-CN-MBE was found to be readily self-assembled into colloidal nanoparticles as a result of reprecipitation when

water was added as a nonsolvent to its solution ( $2 \times 10^{-5} \text{ mol L}^{-1}$ ) in THF. After the addition of an 80 % volume fraction of water to the THF solution, the suspension was macroscopically homogeneous with no precipitates but had a slightly off-white turbidity as a result of light scattering from the nanoparticles<sup>[3]</sup> (Figure 1 a).

Just as previously reported for CN-MBE,<sup>[4]</sup> the absorption spectrum of Py-CN-MBE colloidal nanoparticles was found to be red-shifted and broad-tailed, with an additional shoulder band at 415 nm (Figure 1 c). It has already been shown that these absorption characteristics are a consequence of molecular planarization and *J*-type aggregation in the colloidal nanoparticles.<sup>[4,5,17]</sup> Although the conformation of the Py-CN-MBE molecules (as well as of CN-MBE) is so twisted in the solution state (see Figure S1 in the Supporting Information) that it is virtually nonfluorescent, their aggregation in the colloidal nanoparticles results in a dramatic “turn-on” of fluorescence emission (see Figure 1 e). The presence of the strongly fluorescent Py-CN-MBE nanoparticles in the colloidal suspension is indicated by the Mie scattering<sup>[12]</sup> in the absorption spectrum (Figure 1 c), and was directly confirmed with field-emission scanning electron microscopy (FE-SEM). The SEM image in the inset of Figure 1 c clearly shows that the Py-CN-MBE nanoparticles obtained as a result of the addition of 80 % volume fractions of water to the THF solution are very fine spheres with a mean diameter of 30–40 nm.

Interestingly and surprisingly, it was found that Py-CN-MBE nanoparticles can be generated directly in the polymer film either by using thermal treatment or with the VDSA method. In this study, we adopted the latter method because of its versatility for pattern generation. A Py-CN-MBE-doped thin polymer film was spin-coated from a filtered solution (3.0 wt %) of Py-CN-MBE (5.0 wt % with respect to PMMA) and poly(methyl methacrylate) (PMMA) in 1,2-dichloroethane. Initially, the spin-coated film was smooth and uniform without any discernible nanosized objects (Figure 1 b, left). After exposing the film to dichloromethane vapor for 20 s, however, the vapor-exposed region of the film was found to exhibit very slightly off-white turbidity (Figure 1 b, right), as shown in the colloidal Py-CN-MBE nanoparticle suspension. The UV/Vis absorption spectrum of the vapor-exposed PMMA film (Figure 1 b) was identical to that of the colloidal nanoparticles (Figure 1 d), with red-shifted and shoulder band characteristics.<sup>[18]</sup> These observations imply that Py-CN-MBE nanoparticles are generated in the PMMA matrix. The SEM image in the inset of Figure 1 d shows that fine spherical Py-CN-MBE nanoparticles with a mean diameter of about 30 nm are uniformly distributed over the surface of the vapor-exposed film.

The supramolecular self-assembly of Py-CN-MBE leading to the formation of spherical nanoparticles is accompanied by dramatic fluorescence changes. Py-CN-MBE in dilute THF solution exhibits barely detectable blue fluorescence ( $\lambda_{\text{max}} = 457 \text{ nm}$ ), whereas the nanoparticle suspension exhibits sky-blue emission ( $\lambda_{\text{max}} = 481 \text{ nm}$ ) with an extremely high fluorescence intensity (increased by a factor of approximately 62; see Figure 1 e and the inset photo). Similarly, the blue emission ( $\lambda_{\text{max}} = 464 \text{ nm}$ ) of the molecularly dispersed Py-

[\*] B.-K. An, Prof. S. Y. Park  
School of Materials Science and Engineering  
ENG445, Seoul National University  
San 56-1, Shillim-dong, Kwanak-ku, Seoul 151-744 (Korea)  
Fax: (+82) 2-886-8331  
E-mail: parksy@snu.ac.kr  
Prof. S.-K. Kwon  
School of Nano and Advanced Materials Engineering and ERI  
Gyeongsang National University  
Jinju 660-701 (Korea)

[\*\*] This work was supported by the Korea Science and Engineering Foundation (KOSEF) through the National Research Laboratory. Program funded by the Ministry of Science and Technology (No. 2006-03246).

Supporting information for this article is available on the WWW under <http://www.angewandte.org> or from the author.



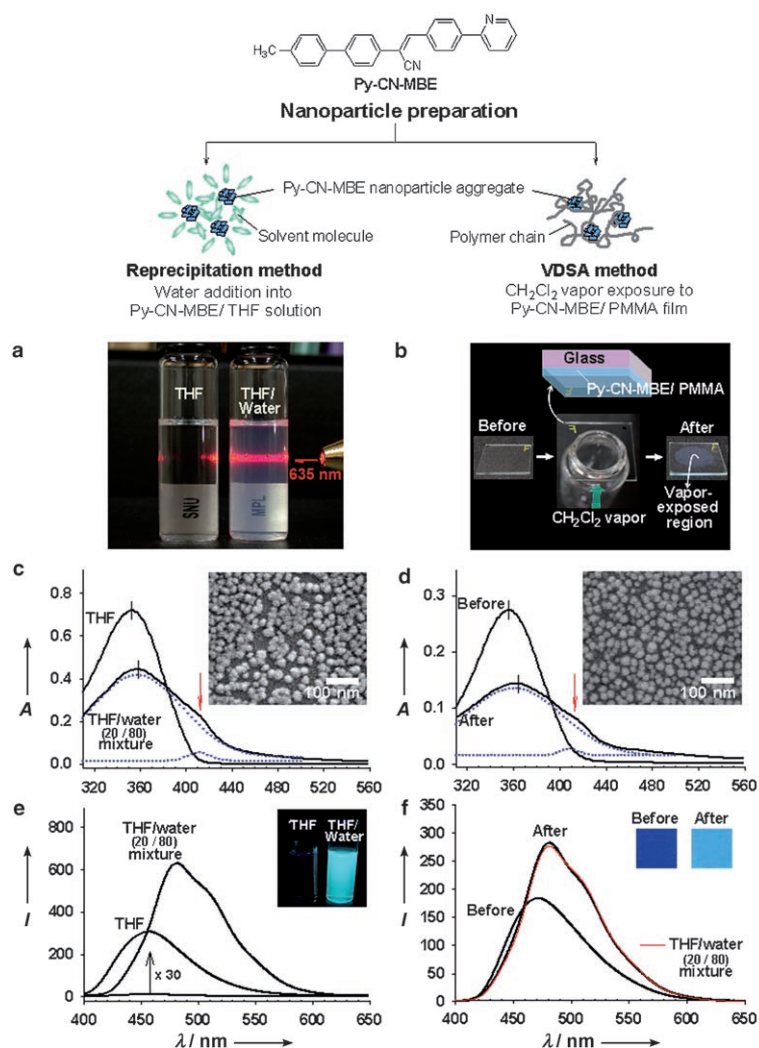


**Figure 1.** Preparation of the Py-CN-MBE nanoparticles. A) Photograph of the Py-CN-MBE solution ( $2 \times 10^{-5} \text{ mol L}^{-1}$ ) in THF and THF/water (20:80 vol %). B) Photographs of the Py-CN-MBE/poly(methyl methacrylate) (PMMA) film before and after exposure to dichloromethane vapor. C, D) UV/Vis absorption spectra of the Py-CN-MBE solution and the Py-CN-MBE/PMMA film after nanoparticle formation. Blue dotted lines show the peak separation of Py-CN-MBE nanoparticles in the case of 80% water addition and exposure to dichloromethane vapor for 20 s. Insets: SEM images of the Py-CN-MBE colloidal nanoparticles obtained with the precipitation method and the VDSA process, respectively. E, F) Photoluminescence (PL) spectra of the Py-CN-MBE solution and the Py-CN-MBE/PMMA film after nanoparticle formation. Insets: the fluorescence emission changes of the Py-CN-MBE solution and the Py-CN-MBE/PMMA film after nanoparticle formation under illumination by UV light at 365 nm.

CN-MBE/PMMA film becomes sky-blue ( $\lambda_{\text{max}} = 482 \text{ nm}$ ) after the generation of nanoparticles with the VDSA method (see Figure 1f and the inset photos). Notably, the blue emission from unaggregated Py-CN-MBE is stronger in solid solution (that is, in situ) than in liquid solution (see Figure 1e and f). This is most likely due to suppression of the vibrational and rotational relaxations in the rigid matrix.<sup>[19]</sup>

To use the VDSA technique to achieve fine patterning of the FON assembly on the solid substrate, we designed the Py-CN-MBE molecule, which includes a pyridine unit as a modulator for use in the VDSA process. The N atoms in the

pyridine rings are readily protonated, so Py-CN-MBE can form bulky quaternary salts with counterpart ions through photochemical reactions.<sup>[20]</sup> We anticipated that this quaternization process of the pyridyl units could eliminate the self-assembling capability of the Py-CN-MBE molecules because of the bulkiness of the pyridine salt groups (Figure 2), and also that the generation of Py-CN-MBE nanoparticles by the VDSA process could be selectively frustrated to give a patterned array of nanoparticles by combining this process with a lithographic photoacid generation process.

On the basis of these considerations, we tested our approach with the procedure illustrated in Figure 3. A Py-CN-MBE-doped film was spin-coated from a filtered solution (3.0 wt %) of Py-CN-MBE (5.0 wt % with respect to PMMA), a photoacid generator (PAG; triphenylsulfonium trifluoromethanesulfonate,  $\lambda_{\text{max,abs}} = 250 \text{ nm}$ ; 3 equiv of Py-CN-MBE) that releases protons ( $\text{H}^+$ ) and counterions ( $\text{X}^- = \text{CF}_3\text{SO}_3^-$ ) upon exposure to UV light, and PMMA in 1,2-dichloroethane (step A). The resulting film exhibited blue fluorescence emission and contained no aggregates (see the photo in Figure 3a and the SEM image in Figure 3b). The film was then exposed to 254-nm UV light ( $1.2 \text{ mW cm}^{-2}$ ) for 1 min through a photomask (step B). The irradiation with UV light gave rise to the transformation of the neutral form (Py-CN-MBE) into the quaternary salt form ( $\text{Py}^+\text{HX}^-$ -CN-MBE) in the illuminated regions of the film. The photo in Figure 3c shows that the blue fluorescent emission of neutral Py-CN-MBE molecules is converted into green fluorescent emission by the quaternization process (see the Figure S3 in the Supporting Information). This change in the color of the fluorescence emission is caused by the narrowing of the optical bandgap that arises as a result of the intramolecular charge transfer that occurs upon protonation of the pyridine rings,<sup>[21]</sup> which is in accordance with the results of semiempirical calculations for neutral Py-CN-MBE (7.7 eV) and protonated Py-CN-MBE (5.0 eV). It was also observed that the film morphology was unchanged (see SEM image in Figure 3d) by the quaternization of the Py-CN-MBE molecules. To generate nanoparticles in the regions of neutral Py-CN-MBE by using the

VDSA process, the UV-treated film was exposed to dichloromethane vapors at room temperature (step C). After exposure to the vapor for 20 s, the blue emission of the neutral Py-CN-MBE region became sky-blue (see photo in Figure 3e), which indicates the formation of Py-CN-MBE nanoparticles in that region, whereas there were no changes at all in the green emission region ( $\text{Py}^+\text{HX}^-$ -CN-MBE; see Figure S3 in the Supporting Information). The SEM image in Figure 3f shows that the formation of Py-CN-MBE nanoparticles is strictly localized in the neutral Py-CN-MBE regions and is frustrated in the quaternized Py-CN-MBE regions. The

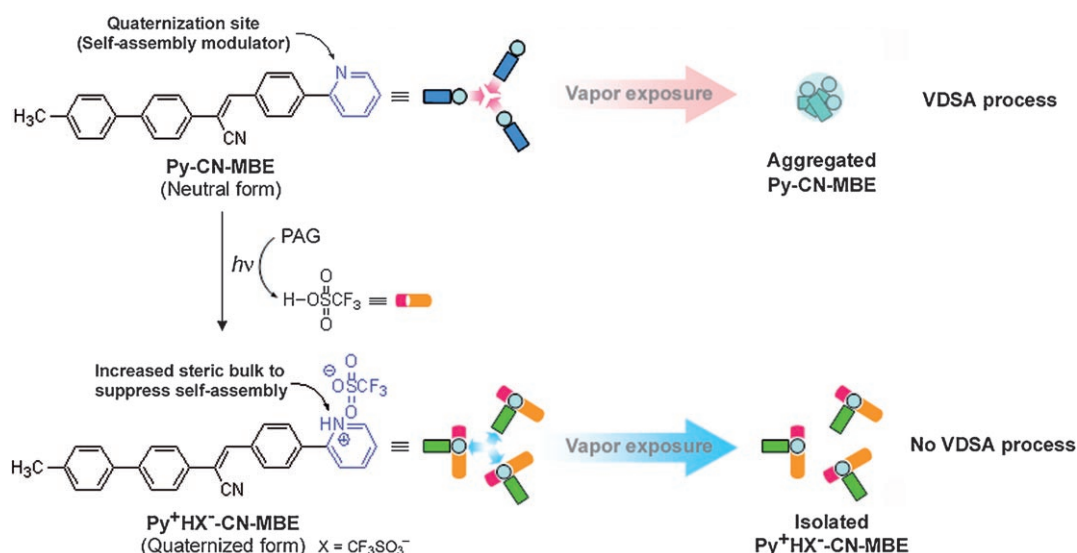


**Figure 2.** Control of the VDSA process by selective frustration of this process in the Py-CN-MBE molecules through the photochemical reaction. The different colors of the Py-CN-MBE cartoon molecules indicate fluorescent color changes of the molecules after an aggregation or a quaternization process. PAG: triphenylsulfonium trifluoromethanesulfonate ( $\lambda_{\text{max,abs}} = 250 \text{ nm}$ ).

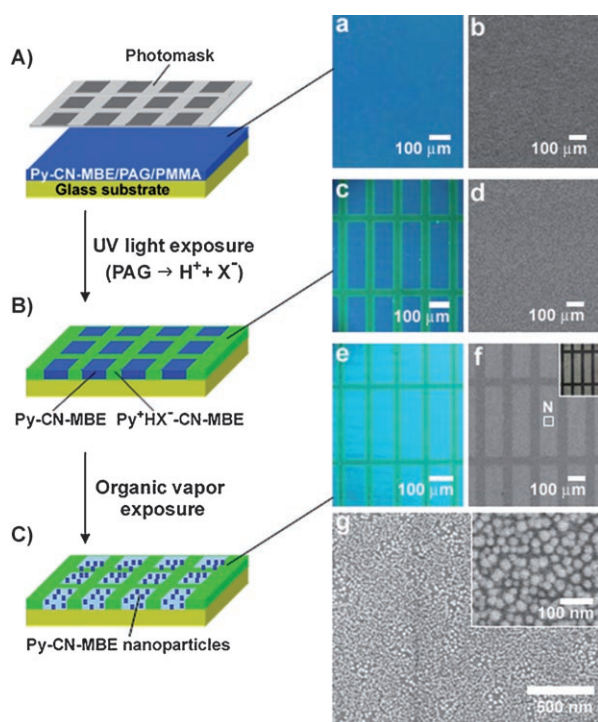


**Figure 3.** Photopatterned array of Py-CN-MBE nanoparticles. A–C) Schematic diagram of the procedure for photopatterning Py-CN-MBE nanoparticles. a–g) Fluorescence emission and SEM images at each step. The inset photo in (f) shows a microscope image of the patterned array of Py-CN-MBE nanoparticles, obtained with a platinum-sputtering treatment.

magnified SEM image of the region N in Figure 3 f shows that the nanoparticles formed in the neutral Py-CN-MBE regions are very fine unimodal spheres with a mean diameter of approximately 30 nm (Figure 3 g). More sophisticated photopatterned arrays of Py-CN-MBE nanoparticles were also

obtained with the procedure described above (see Figure S4 in the Supporting Information).

In conclusion, we have devised a simple, rapid, and reliable method for the fabrication of photopatterned assemblies of FONs on the surfaces of solid substrates, which combines bottom-up VDSA and top-down photochemical lithography. This technology has the potential to eliminate the difficulties of transferring preformed colloidal FONs onto fixed locations on substrates, thereby opening up a new approach to the realization of practical optoelectronic nano-device applications of FONs.

### Experimental Section

The details of the Py-CN-MBE synthesis are described in the Supporting Information. The UV/Vis absorption and fluorescence emission spectra were recorded on an HP 8452A and a Shimadzu RF-500 spectrofluorophotometer, respectively. FE-SEM images were acquired on a JSM-6330F microscope (JEOL). The fluorescence images were obtained with a digital camera (Nikon-Coolpix 995) and a microscope (Leica) under illumination at 365 nm. The optimized geometry and bandgaps of neutral and protonated Py-CN-MBE in the gas phase were calculated by using the AM1 parameterization in the HyperChem 5.0 program (Hypercube).

Preparation of Py-CN-MBE nanoparticles through either the reprecipitation method or the VDSA method:

**Reprecipitation method:** Distilled water was regularly injected with a syringe pump into the Py-CN-MBE/THF solution with vigorous stirring at room temperature. Before injection of the distilled water, the water and the Py-CN-MBE solution were filtered with a membrane filter of pore size 0.2  $\mu\text{m}$ . The SEM image of the Py-CN-MBE nanoparticles in the inset of Figure 1 c was acquired by dropping the suspension of Py-CN-MBE nanoparticles onto a slide glass.

**VDSA method:** A Py-CN-MBE-doped polymer film was spin-coated (3000 rpm, film thickness approximately 200 nm) from a filtered solution (3.0 wt %) of Py-CN-MBE (5.0 wt % with respect to PMMA) and PMMA (weight-average molecular weight  $M_w = 120000$ ) in 1,2-dichloroethane. As shown in Figure 1 b, the resulting

film was then turned upside down and placed on top of the spout of a 20-mL vial to which dichloromethane (1 mL) was added at room temperature over about 20 s.

Received: October 13, 2006

Published online: January 16, 2007

**Keywords:** fluorescence · nanoparticles · polymers · self-assembly · supramolecular chemistry

- [1] H. Kasai, H. Kamatani, S. Okada, H. Oikawa, H. Matsuda, H. Nakanishi, *Jpn. J. Appl. Phys.* **1996**, 34, L221–L223.
- [2] J. D. Luo, Z. L. Xie, J. W. Y. Lam, L. Cheng, H. Y. Chen, C. F. Qiu, H. S. Kwok, X. W. Zhan, Y. Q. Liu, D. B. Zhu, B. Z. Tang, *Chem. Commun.* **2001**, 1740–1741.
- [3] H. B. Fu, J. N. Yao, *J. Am. Chem. Soc.* **2001**, 123, 1434–1439.
- [4] B. K. An, S. K. Kwon, S. D. Jung, S. Y. Park, *J. Am. Chem. Soc.* **2002**, 124, 14410–14415.
- [5] S. J. Lim, B. K. An, S. D. Jung, M. A. Chung, S. Y. Park, *Angew. Chem.* **2004**, 116, 6506–6510; *Angew. Chem. Int. Ed.* **2004**, 43, 6346–6350.
- [6] L. Xi, H. B. Fu, W. S. Yang, J. N. Yao, *Chem. Commun.* **2005**, 492–494.
- [7] A. D. Peng, D. B. Xiao, Y. Ma, W. S. Yang, J. N. Yao, *Adv. Mater.* **2005**, 17, 2070–2073.
- [8] M. Han, M. Hara, *J. Am. Chem. Soc.* **2005**, 127, 10951–10955.
- [9] F. Wang, M. Y. Han, K. Y. Mya, Y. B. Wang, Y. H. Lai, *J. Am. Chem. Soc.* **2005**, 127, 10350–10355.
- [10] N. Makarava, A. Parfenov, I. V. Baskakov, *Biophys. J.* **2005**, 89, 572–580.
- [11] Y. Y. Sun, J. H. Liao, J. M. Fan, P. T. Chou, C. H. Shen, C. W. Hsu, L. C. Chen, *Org. Lett.* **2006**, 8, 3713–3716.
- [12] D. Horn, J. Rieger, *Angew. Chem.* **2001**, 113, 4460–4492; *Angew. Chem. Int. Ed.* **2001**, 40, 4330–4361.
- [13] a) S. A. Vitale, J. L. Katz, *Langmuir* **2003**, 19, 4105–4110; b) F. Ganachaud, J. L. Katz, *ChemPhysChem* **2005**, 6, 209–216.
- [14] R. C. Hayward, D. A. Saville, I. A. Aksay, *Nature* **2000**, 404, 56–59.
- [15] F. Hua, J. Shi, Y. Lvov, T. Cui, *Nano Lett.* **2002**, 2, 1219–1222.
- [16] a) S. Magdassi, M. Ben-Moshe, *Langmuir* **2003**, 19, 939–942; b) L. Zhao, Z. X. Lei, X. R. Li, S. B. Li, J. Xu, B. Peng, W. Huang, *Chem. Phys. Lett.* **2006**, 420, 480–483.
- [17] B. K. An, D. S. Lee, J. S. Lee, Y. S. Park, H. S. Song, S. Y. Park, *J. Am. Chem. Soc.* **2004**, 126, 10232–10233.
- [18] For details of UV/Vis absorption spectrum monitoring of the generation of Py-CN-MBE nanoparticles by the reprecipitation and VDSA methods, see the Supporting Information (Figure S2).
- [19] Y. Ren, J. W. Y. Lam, Y. Q. Dong, B. Z. Tang, K. S. Wong, *J. Phys. Chem. B* **2005**, 109, 1135–1140.
- [20] a) D. T. McQuade, A. E. Pullen, T. M. Swager, *Chem. Rev.* **2000**, 100, 2537–2574; b) D.-K. Fu, B. Xu, T. M. Swager, *Tetrahedron* **1997**, 53, 15487–15494.
- [21] S. Scheiner, T. Kar, *J. Phys. Chem. B* **2002**, 106, 534–539.